Journal of Microscopy, Vol. 202, Pt 1, April 2001, pp. 72–76.
Received 28 August 2000; accepted 11 October 2000

A single gold particle as a probe for apertureless scanning near-field optical microscopy

T. KALKBRENNER, M. RAMSTEIN, J. MLYNEK & V. SANDOGHDAR
Fachbereich Physik & Optik-Zentrum Konstanz, Fach M696, D-78457 Konstanz, Germany

Key words. Gold nanoparticle, SNOM.

Summary

We report on the fabrication, characterization and application of a probe consisting of a single gold nanoparticle for apertureless scanning near-field optical microscopy. Particles with diameters of 100 nm have been successfully and reproducibly mounted at the end of sharp glass fibre tips. We present the first optical images taken with such a probe. We have also recorded plasmon resonances of gold particles and discuss schemes for exploiting the wavelength dependence of their scattering cross-section for a novel form of apertureless scanning near-field optical microscopy.

1. Introduction

In the conventional configuration of scanning near-field optical microscopy (SNOM) evanescent fields are produced at a subwavelength aperture at the end of a metal-coated sharp dielectric probe (Lewis *et al.*, 1984; Pohl *et al.*, 1984). These fields contain high spatial frequency Fourier components that can be converted into propagating waves if a sample structure is brought close enough to the aperture. This approach, referred to as aperture SNOM, has been extremely successful because the sample is illuminated very locally, and therefore there exists essentially no background. This feature is of invaluable importance for studies of samples with weak signals such as single molecules. Nevertheless, several problems have considerably slowed down the spread of aperture SNOM as a reliable and routine laboratory tool. First, reliable and economic fabrication of probes has presented a big challenge for about a decade and a half. Second, there is a practical lower limit of about 30 nm imposed on the resolution that can be obtained using an aperture (Novotny *et al.*, 1995). This is because the optical radiation at the aperture penetrates into the metallic coating by a finite amount, resulting in an opening that is effectively quite a bit larger than the physical aperture.

Correspondence to: V. Sandoghdar. Tel.: +49 7531 883824; fax: +49 7531 883072; e-mail: vahid.sandoghdar@uni-konstanz.de

Even before these limitations were fully appreciated, there were proposals and reports on other configurations of SNOM. In 1989 scattering of surface plasmons at protrusions in a metallic film were used as probes for imaging a sample in the near field (Fischer & Pohl, 1989). In the first half of the 1990s a few groups reported on SNOM configurations using sharp metallic or dielectric tips as probes (Specht *et al.*, 1992; Inouye & Kawata, 1994; Zenhausern *et al.*, 1994; Gleyzes *et al.*, 1995). More recently, two-photon fluorescence excitation (Sánchez *et al.*, 1999), infrared spectroscopy of polymers (Knoll & Keilmann, 1999) and surface enhanced Raman scattering (SERS) (Stöckle *et al.*, 2000) have also been combined successfully with such tips. In all these experiments one illuminates the sample using far-field optics and detects the light scattered at the junction between the sample and the probe. It is a very demanding task to identify the very small near-field signal from the very large background scattered by the tip shaft and the sample. To improve this situation lock-in techniques commonly are applied whereby the tip–sample distance is modulated. Nevertheless, one often has to fight against spurious distance-dependent signals that persist even after a simple lock-in detection (Labardi *et al.*, 2000).

In summary, although optical resolution in the nanometre range has been reported (Zenhausern *et al.*, 1995) and some careful studies have been made (Aigouy *et al.*, 1999), systematic studies of the imaging mechanisms in apertureless SNOM are still missing in the literature. The main experimental difficulty is a very weak signal on a large background due to a global illumination. Furthermore, although it has been often assumed that only the far extremity of the tip contributes to the signal, the influence of the extended nature of the tips used has not been properly examined. In an ideal experiment one would like to study the interaction of well-characterized and well-controlled probe and sample in a variety of illumination and detection configurations. In this paper we present our attempts in conceiving such an experiment. The key idea is simply to use a single nanoscopic metal particle of known size and material as a local scatterer (Wessel, 1985; Keller *et al.*,

1993; Sugiura *et al*., 1999). The optical resolution in this mode is expected to depend only on the size of the scatterer and its distance from the sample, although field enhancement effects in the near field could also play an important role in the interaction between the probe and the sample. In what follows we describe a method for a reliable fabrication of the desired probes. Next we show preliminary results of SNOM measurements. Then we present the plasmon resonance of an individual gold nanoparticle situated at the end of a fibre tip, and in closing we discuss future plans to take advantage of these resonances as well as second harmonic generation for extracting the near-field signal from the background of far-field illumination.

2. Probe fabrication

We have developed a procedure for placing a single gold nanoparticle at the very end of a tapered optical fibre tip. The advantage of this method is first that in contrast to the case of particles manipulated in optical tweezers (Sugiura *et al*., 1999) our particle is tightly bound to the tip and using shearforce control can be positioned against any surface at will. Second, contrary to the case of a fully metallized probe, the glass fibre tip with a low index of refraction is much more weakly scattering than the region at its end, namely a gold particle. This results in a lower background signal.

The probe preparation as well as SNOM measurements are all done in a set-up consisting of a combined scanning confocal and scanning near-field microscope using the platform of an inverted optical microscope. We start by spin-coating colloidal gold particles of diameter 50 or 100 nm on a microscope cover glass in a manner to obtain a coverage well under a monolayer. As displayed in Fig. 1(a), we then image individual particles in the confocal mode and target one of them to which we approach an optical fibre tip mounted in the SNOM head with a shear-force control. Before mounting the fibre tip in the SNOM it is placed in a solution of polyethylenimine for about 30 min in order to adsorb a monolayer which acts as a glue for our gold particles. Therefore, when the fibre tip establishes contact with a gold nanosphere it lifts the particle, and a probe as shown in Fig. 1(b) is obtained. Typically we then repeat a confocal scan of the same area, verifying that the gold particle is indeed missing (see Fig. 1c). This procedure has the advantage that we can fabricate probes with very well-defined optical properties, namely a single particle of given size and material at the end of a glass fibre tip. In this manner we have produced more than 20 tips with a success rate of nearly 100%.

3. SNOM measurements

Figure 2 shows the arrangement for our apertureless SNOM measurements. The probe is positioned on the optical axis of the inverted microscope. Light from a ring dye laser operating at $\lambda \sim 600$ nm is transmitted through a single mode optical fibre and brought close to the tip at a very large angle so that the junction between the tip and the sample is illuminated uniformly. The distance between the tip and the sample is controlled using shear-force signal from a segmented piezo tube (Barenz *et al*., 1996). The tip and illumination are fixed while the sample is scanned in all three directions by a piezoelectric element. A variable pinhole is used at the Fourier plane of the microscope tube lens to discriminate against the background light.

The sample used in this first experiment was a thin aluminium film containing isolated holes of 3 μm diameter

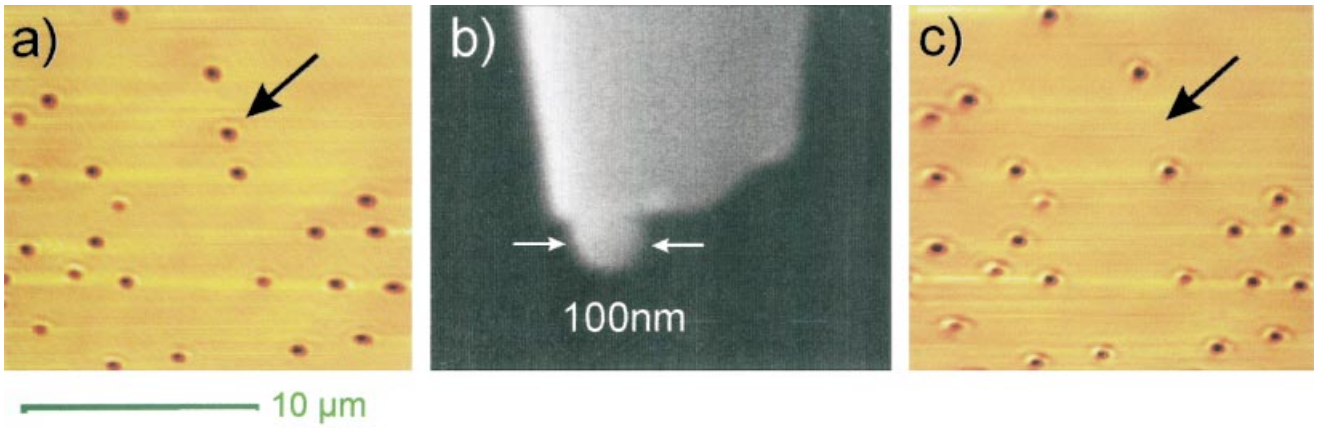

Fig. 1. (a) Confocal scan of individual gold spheres of 100 nm diameter spread on a glass substrate. A fibre tip prepared as described in section 2 has been approached to the particle indicated by the arrow using shear-force control. After establishing contact to the gold sphere the particle has been fixed to the tip. (b) Scanning electron micrograph of the tip after the procedure described in (a). (c) Confocal scan of the same area as in (a), verifying that the chosen particle has left the substrate. Its former position is indicated by an arrow.

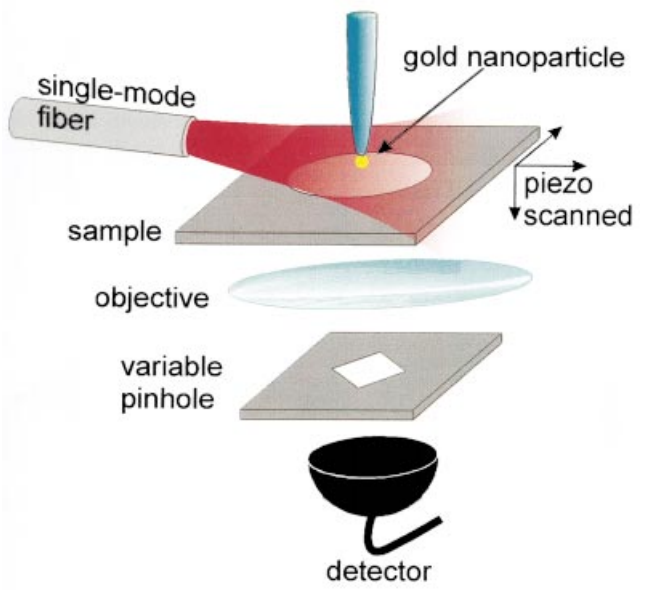

Fig. 2. A single gold particle attached to the end of a sharp optical fibre tip is positioned in front of a sample. The tip–sample combination is illuminated globally using light out of a single mode optical fibre at a very large angle of incidence. The optical signal is collected with a microscope objective and sent to a photomultiplier via a variable pinhole.

on a glass substrate. To fabricate this sample a very low concentration of latex spheres of size 3 μm were first spin-coated on a microscope cover glass that was then coated with about 5–7 nm of aluminium. After removing the latex beads we are left with the final sample. Atomic force microscope measurements verified that the transition between glass and aluminium parts of the sample take place within about 10 nm and that the edges are all very sharp.

Figure 3(a) displays the topography signal from a hole in the aluminium film. Figure 3(b) displays an image that was taken when the tip was more than 100 μm away from the sample. The signal on the detector increases as the hole in the sample is scanned against the pinhole, which was set to be about 30 μm. When the tip is engaged we obtain the image in Fig. 3(c). In Fig. 3(d) we show the result of subtracting 3(b) from 3(c). The location of the hole is superposed on Figs 3(c) and 3(d) in order to facilitate a more quantitative scrutiny of the scans. Figures 3(e) and (f) plot two cross-sections from 3(d), as well as fit functions $\tanh[(x - x_0)/l]$, where l and x_0 are free parameters. For each fit we have determined the width over which the signal drops from its 90% value to 10% and have found edge sharpness of 200 nm and 100 nm, respectively. This is typical of cross-sections elsewhere in the image, as well as in other images taken under similar conditions. We note that the cross-sections shown were laid in an area where the stray background did not have a large contribution, so that the act of subtracting intensities in images (b) and (c) does not introduce false results. This is not true for the lower region of the hole, where interference between the background signal and that of the tip becomes important. In order to get around this problem we plan to take advantage of the wavelength dependence in the scattering cross-section of a gold nanosphere, as elaborated in the next section.

4. Plasmon resonance of a single gold particle

The scattering cross-sections of small particles depend strongly on their size, morphology and index of refraction (Bohren & Huffman, 1983). In particular, gold and silver nanoparticles are known to show pronounced resonances in the visible range (Kreibig & Vollmer, 1995). These so-called plasmon resonances are understood as the result of collective oscillations of the free electrons upon excitation by the appropriate optical field. The details of such a resonance, especially its linewidth, reveal quite a bit of information about the internal dynamics of the electronic motion and are therefore of current interest (Lamprecht *et al.*, 2000). Recently, plasmon resonances of individual gold particles in a dielectric matrix were recorded using aperture SNOM (Klar *et al.*, 1998). In Fig. 4 we present measurements of the plasmon resonances of a single gold nanoparticle of 100 nm in diameter attached to a tip. The general trend of the spectrum agrees very well with the expectations of the Mie theory (see solid line), but more quantitative measurements are needed to study the influence of the nanoscopic environment such as a glass tip on these resonances. In the context of apertureless SNOM we plan to use this characteristic wavelength dependence of plasmon resonances as a signature to identify the signal of a gold particle, and therefore discriminate against background.

5. Conclusion

We have reported on a new arrangement for apertureless SNOM based on local scattering. We have described a reliable procedure for fabrication of probes consisting of a single gold nanoparticle at the very extremity of a sharp glass fibre tip. First optical measurements show resolution in the order of 100 nm, as expected from the size of the gold particles used. Future work will focus on repeating these measurements with smaller gold particles to improve the resolution. It will be also interesting to study the polarization dependence of the images (Betzig *et al.*, 1992). A very promising approach consists of introducing a wavelength dependence into scattering-based apertureless SNOM. Here we plan to take advantage of the plasmon resonances of gold particles and possibly second harmonic generation at the junction between the probe and the sample (Zayats &

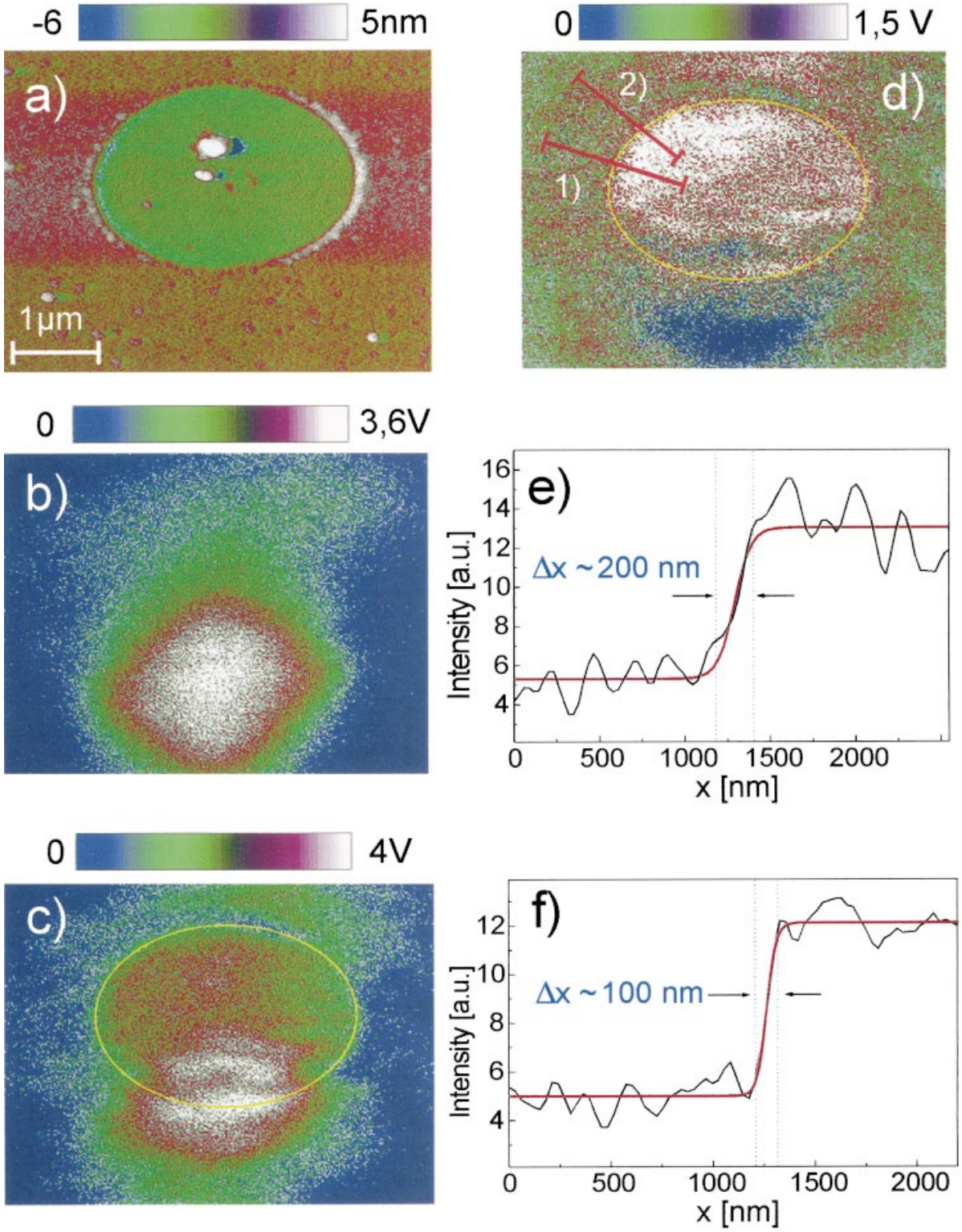

Fig. 3. (a) Topography signal showing a 3 µm hole in an aluminium film of thickness 7 nm. (b) Optical signal recorded with retracted tip. (c) Optical signal with the tip engaged. (d) The result of signal (b) subtracted from signal (c). In (c) and (d) the location of the hole is indicated by yellow lines. (e) Cross-section (1) in (d) showing an edge sharpness of 200 nm. (f) Cross-section (2) in (d) showing an edge sharpness of 100 nm. A fit using a hyperbolic tangent $\tanh[(x - x_0)/l]$ is used to quantify the edge sharpness in these cuts.

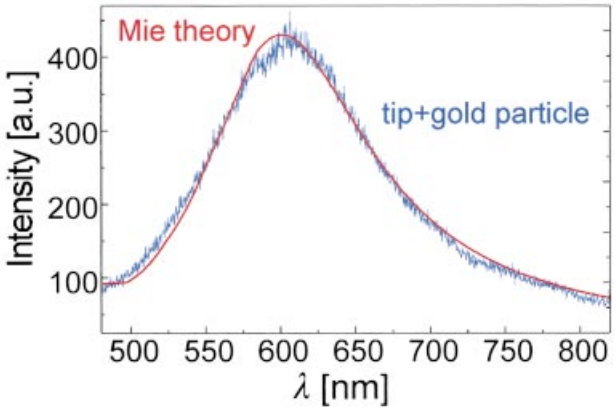

Fig. 4. Scattering spectrum of a gold sphere of 100 nm diameter attached to a fibre tip. The tip was illuminated by a white light source and the scattered intensity was analysed by a spectrometer and a cooled CCD camera. The solid line shows the resonance of a 100-nm gold particle predicted by Mie theory.

Sandoghdar, 2000) to favour the near-field signal stemming from the gold particle and to discriminate against the global background scattering. In closing, we note that as already pointed out by Sugiura *et al*. (1999), a single gold nanoparticle holds the very important promise for three-dimensional near-field imaging of biological samples.

Acknowledgements

We acknowledge financial support from the Land Baden-Württemberg (Optik-Zentrum Konstanz). We thank S. Kühn for manufacturing the variable pinhole used in this experiment and A. Zayats and G. Decher for fruitful discussion. T. Kalkbrenner acknowledges a fellowship from the Carl-Zeiss-Schott-Förderstiftung.

References

Aigouy, L., Lahrech, A., Grésillon, S., Cory, H., Boccara, A.C. & Rivoal, J.C. (1999) Polarization effects in apertureless scanning near-field optical microscopy: an experimental study. *Opt. Lett*. **24**, 187–189.

Barenz, J., Hollricher, O. & Marti, O. (1996) An easy-to-use nonoptical shear-force distance control for near-field optical microscopes. *Rev. Sci. Instrum*. **67**, 1912–1916.

Betzig, E., Trautman, J.K., Weiner, J.S., Harris, T.D. & Wolfe, R. (1992) Polarization contrast in near-field scanning optical microscopy. *Appl. Opt*. **31**, 4563–4568.

Bohren, C.E. & Huffman, D.R. (1983) *Absorption and Scattering of Light by Small Particles*. John Wiley & Sons, Chichester.

Fischer, U.C. & Pohl, D.W. (1989) Observation of single-particle plasmons by near-field optical microscopy. *Phys. Rev. Lett*. **62**, 458–461.

Gleyzes, P., Boccara, A.C. & Bachelot, R. (1995) Near field optical microscopy using a metallic vibrating tip. *Ultramicroscopy*, **57**, 318–322.

Inouye, Y. & Kawata, S. (1994) Near-field scanning optical microscope with a metallic probe tip. *Opt. Lett*. **19**, 159–161.

Keller, O., Bozhevolnyi, S. & Xiao, M. (1993) On the resolution limit of optical near-field microscopy. *Near Field Optics* (ed. by D. W. Pohl and D. Courjon), pp. 229–237. Kluwer Academic Press, Dordrecht.

Klar, T., Perner, M., Gross, S., von Plessen, G., Spirk, I.W. & Feldmann, J. (1998) Surface-plasmon resonances in single metallic nanoparticles. *Phys. Rev. Lett.* **80**, 4249–4252.

Knoll, B. & Keilmann, F. (1999) Near-field probing of vibrational absorption for chemical microscopy. *Nature*, **399**, 134–137.

Kreibig, U. & Vollmer, M. (1995) *Optical Properties of Metal Clusters*. Springer, Berlin.

Labardi, M., Patanè, S. & Allegrini, M. (2000) Artifact-free nearfield optical imaging by apertureless microscopy. *Appl. Phys. Lett*. **77**, 621–623.

Lamprecht, B., Schider, G., Lechner, R.T., Ditlbacher, H., Krenn, J.R., Leitner, A. & Aussenegg, F.R. (2000) Metal nanoparticle gratings: influence of dipolar particle interactions on the plasmon resonance. *Phys. Rev. Lett.* **84**, 4721–4724.

Lewis, A., Isaacson, M., Harootunian, A. & Murray, A. (1984) Development of a 500Å spatial resolution light microscope. *Ultramicroscopy*, **13**, 227–231.

Novotny, L., Pohl, D.W. & Hecht, B. (1995) Scanning near-field optical probe with ultrasmall spot size. *Opt. Lett*. **20**, 970–972.

Pohl, D.W., Denk, W. & Lanz, M. (1984) Optical stethoscopy: image recording with resolution λ/20. *Appl. Phys. Lett.*, **44**, 651–653.

Sánchez, E., Novotny, L. & Xie, X.S. (1999) Near-field fluorescence microscopy based on two-photon excitation with metal tips. *Phys. Rev. Lett.*, **82**, 4014–4017.

Specht, M. & Pedarnig, J.D., HeckI, W.M. & Hänsch, T.W. (1992) Scanning plasmon near-field microscope. *Phys. Rev. Lett*. **68**, 476–479.

Stöckle, R.M., Sun, Y.D., Deckert, V. & Zenobi, R. (2000) Nanoscale chemical analysis by tipenhanced Raman spectroscopy. *Chem. Phys. Lett*. **318**, 131–136.

Sugiura, T., Kawata, S. & Okada, T. (1999) Fluorescence imaging with a laser trapping scanning near-field optical microscope. *J. Microsc*. **194**, 291–294.

Wessel, J.J., (1985) Surface-enhanced optical microscopy. *J. Opt. Soc. Am. B* **B2**, 1538.

Zayats, A. & Sandoghdar, V. (2000) Apertureless scanning near-field second-harmonic microscopy. *Opt. Comm*. **178**, 245–249.

Zenhausern, F., Martin, Y. & Wickramasinghe, H.K. (1995) Scanning interferometric apertureless microscopy: optical imaging at 10A resolution. *Science*, **269**, 1083–1085.

Zenhausern, F., O'Boyle, M.P. & Wickramasinghe, H.K. (1994) Apertureless near-field optical microscope. *Appl. Phys. Lett*. **65**, 1623–1625.